Structural Engineering and Mechanics, *Vol. 58, No. 3 (2016) 515-532*
DOI: http://dx.doi.org/10.12989/sem.2016.58.3.515

Post-buckling responses of elastoplastic FGM beams on nonlinear elastic foundation

Thanh-Huong Trinh[1a], Dinh-Kien Nguyen[2b], Buntara S. Gan[*1] and S. Alexandrov[3c]

[1]*Department of Architecture, College of Engineering, Nihon University, Koriyama, Fukushima, 963-8642 Japan*
[2]*Department of Solid Mechanics, Institute of Mechanics, Vietnam Academy of Science and Technology, 18 Hoang Quoc Viet, Hanoi, Vietnam*
[3]*Laboratory of Fracture Mechanics, Institute for Problems in Mechanics, Moscow 11926, Russia*

(Received July 9, 2015, Revised February 11, 2016, Accepted February 29, 2016)

Abstract. The elastoplastic response of functionally graded material (FGM) beams resting on a nonlinear elastic foundation to an eccentric axial load is investigated by using the finite element method. The FGM is assumed to be formed from ceramic and metal phases with their volume fraction vary in the thickness direction by a power-law function. A bilinear elastoplastic behavior is assumed for the metallic phase, and the effective elastoplastic properties of the FGM are evaluated by Tamura-Tomota-Ozawa (TTO) model. Based on the classical beam theory, a nonlinear finite beam element taking the shift in the neutral axis position into account is formulated and employed in the investigation. An incremental-iterative procedure in combination with the arc-length control method is employed in computing the equilibrium paths of the beams. The validation of the formulated element is confirmed by comparing the equilibrium paths obtained by using the present element and the one available in the literature. The numerical results show that the elastoplastic post-buckling of the FGM beams is unstable, and the post-buckling strength is higher for the beams associated with a higher ceramic content. Different from homogeneous beams, yielding in the FGM beam occurs in the layer near the ceramic layer before in the layer near metal surface. A parametric study is carried out to highlight the effect of the material distribution, foundation support and eccentric ratio on the elastoplastic response of the beams.

Keywords: FGM beam; elastoplastic behavior; nonlinear elastic foundation; eccentric axial load; nonlinear finite element analysis

1. Introduction

Analysis of beams resting on elastic foundation is an important topic in the field of structural mechanics, and it has been drawn much attention by many researchers for a long time. A large number of studies of beams on elastic foundation are referred to in the excellent monograph by

∗Corresponding author, Professor, E-mail: buntara@arch.ce.nihon-u.ac.jp
[a]Ph.D. Candidate, M.Sc., E-mail: thanhhuong31@gmail.com
[b]Ph.D., E-mail: ndkien@imech.ac.vn
[c]Professor, E-mail: sergey_alexandrov@spartak.ru

http://www.techno-press.org/?journal=sem&subpage=8 ISSN: 1225-4568 (Print), 1598-6217 (Online)

Hetényi (1946). Recent contributions that are most relevant to the present topic are briefly discussed herein. Zhaohua and Cook (1983) studied the bending problem of beams on a two-parameter elastic foundation by using the exact interpolation in the derivation of the stiffness matrix. Chaht *et al.* (2015) addressed theoretical bending and buckling behaviors of size-dependent nanobeams made of FGM on the basis of the nonlocal elastic continuum model. Razaqpur and Shah (1991) derived the exact stiffness matrix and nodal force vector for assessing the deflection and internal forces of beams resting on a two-parameter elastic foundation. Chegenizadeh *et al.* (2014) investigated FGM beams on the elastic and plastic soil mediums subjected to dynamic and static loadings by using commercial finite element software ABAQUS. Budkowska and Szymczak (1997) used a simple finite element model in studying the post-buckling behavior of beams partially embedded in a Winkler foundation. Kounadis *et al.* (2006) have shown that the post-buckling behavior of elastic beams resting on a Winkler foundation is stable. The equilibrium paths, computed by Patel *et al.* (1999), Nguyen *et al.* (2004) by using the finite element method, have also confirmed the stable behavior in the post-buckling region of axially loaded beams resting on a two-parameter elastic foundation. However, due to the increase of the critical load by the elastic foundation support, the stress in beams on an elastic foundation may exceed yield stress when the deflection is still very small, even before buckling. Thus, the effect of plastic deformation is an important factor for the buckling behavior of beams resting on the elastic foundation. In this line of work, based on Hill's variational principle Cheb and Neal (1984) developed a finite element procedure for investigating the buckling and post-buckling behavior of elastic-plastic beams resting on a nonlinear elastic foundation. They have then shown that the post-buckling behavior of the elastic-plastic beams on the foundation is unstable, and the maximum load that the beams can withstand is sensitive to the imperfection and the foundation stiffness. Also using a finite element procedure, Nguyen and his co-workers have confirmed that the post-buckling behavior of beams on elastic foundation subjected to an eccentric axial load is unstable, and the post-buckling strength, measured in term of a ratio between the axial load and the critical load, increases with an increment in the foundation stiffness.

The new type of composite developed recently, namely functionally graded material (FGM) has high potential to use as a structural material. This composite, usually formed from metals and ceramics, has no thermal stress concentration and delaminating problems as often met in conventional composites. Many investigations have been reported on the behavior of FGM structures subjected to static or dynamic loadings. Concerning to analysis of FGM beams, Chakraborty *et al.* (2003) derived a first-order shear deformable beam element for investigating the thermoelastic behavior of FGM beams. Based on the third-order shear deformation beam theory, Kadoli *et al.* (2008) derived a beam element for studying the static behavior of FGM beams under ambient temperature. Singh and Li (2009) proposed a model for computing buckling loads of non-uniform axially FGM columns by approximating the column by another one with piecewise uniform geometric and material properties. Kang and Li (2009, 2010) took the shift in the neutral axis position into account in their derivation of the expressions for tip response of a cantilever FMG Euler-Bernoulli beam subjected to a transverse end force or an end moment. Nguyen (2013, 2014) derived the co-rotational beam elements for large displacement analysis of tapered beams made of axially or transversely FGM. Also using the finite element method, Nguyen and Gan (2014), Nguyen *et al.* (2014) investigated the geometrically nonlinear behavior of beams and frames made of transversely FGM.

Analysis of elastoplastic FGM structures in general and FGM beam, in particular, has not been carried out sufficiently by researchers. Only a few recent publications on this topic can be found in

the literature. Gunes *et al.* (2011) employed the finite element code LS-DYNA to study the elastoplastic response of FG circular plates under low-velocity impact loads. Jahromi *et al.* (2012) used a bilinear tress-strain relationship in modeling the elastoplastic behavior of an FG rotating disk. The stress field of the disk is then computed with the aid of the commercial finite element package ABAQUS. Huang and Han (2014) assumed a multi-linear hardening elastoplastic material to study the elastoplastic buckling of FG cylindrical shells subjected to the axial load. Also using the multi-linear hardening elastoplastic material model, Zhang *et al.* (2015) studied the buckling behavior of elastoplastic FG cylindrical shells under a combination of the axial compressive load and external pressure.

The present article aims to investigate the elastoplastic response of FGM beams resting on a nonlinear elastic foundation under an eccentric axial load. The FGM is assumed to be formed from ceramic and metal whose volume fraction varying in the thickness direction by a power-law function. A bilinear tress-strain relationship with isotropic hardening is assumed for the metal, and the effective elastoplastic properties of the FGM are evaluated by a model proposed by Tamura-Tomota-Ozawa (Tamura *et al.* 1973), which is called TTO model herein. Based on the classical beam theory, a nonlinear two-node beam element is formulated by adopting the nonlinear von Kármán strain-displacement relationship, and taking the shift in the neutral axis position into account. An incremental-iterative procedure in combination with the arc-length control method is employed in solving the nonlinear equilibrium equations and computing the load-displacement curves. Numerical investigations are presented in detail for cantilever and simply supported beams. The effect of the material distribution, foundation support, plastic deformation on the behavior of the beam is investigated. The influence of eccentric ratio of the behavior of the beam is also examined and highlighted.

2. FGM beam on elastic foundation

Fig. 1 shows a cantilever FGM beam with length L, height h, width b, resting on a nonlinear elastic foundation under an eccentric axial load P. The beam material assumed to be formed from ceramic and metal with the volume fraction of constituent materials varies in the beam thickness according to a power-law function

$$V_c = \left(\frac{z}{h} + \frac{1}{2}\right)^n; \quad V_c + V_m = 1 \tag{1}$$

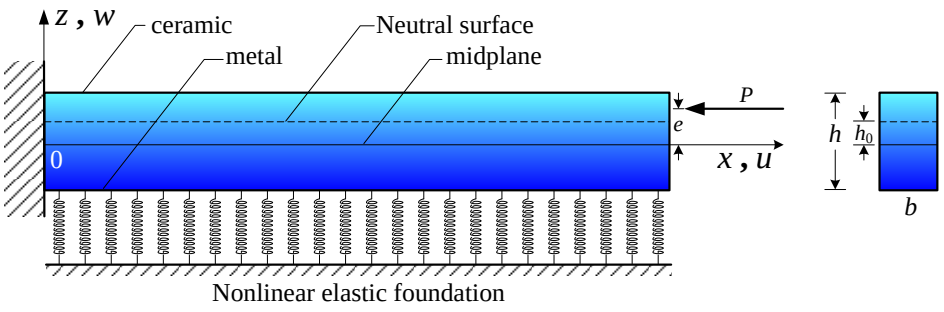

Fig. 1 Cantilever FGM beam on a nonlinear elastic foundation under eccentric axial load

where z is the transverse coordinate; V_c and V_m are respectively the volume fractions of ceramic and metal, and n is the non-negative volume fraction exponent. In Eq. (1) and hereafter, the lower subscripts 'c' and 'm' stand for 'ceramic' and 'metal', respectively.

The linear elastic behavior of FGM is described by Hooke's law, and its effective material properties can be evaluated by micromechanics models used in conventional composites. The elastoplastic behavior of ceramic/metal FGMs is widely described by TTO model (Tamura *et al.* 1973). According to the TTO model, the ceramic constituent is assumed to be elastic. Material flow of FGMs mainly arose by plastic flow of the metallic constituent, and the effective elastoplastic properties of FGMs are evaluated as (Jin *et al.* 2003)

$$E(z)=\frac{\left(\frac{q+E_c}{q+E_m}E_mV_m+E_cV_c\right)}{\left(\frac{q+E_c}{q+E_m}V_m+V_c\right)}$$
$$\sigma_Y(z)=\sigma_{Ym}\left(V_m+\frac{q+E_m}{q+E_c}\frac{E_c}{E_m}V_c\right) \tag{2}$$
$$E_t(z)=\frac{\left(\frac{q+E_c}{q+E_0}E_0V_m+E_cV_c\right)}{\left(\frac{q+E_c}{q+E_0}V_m+V_c\right)}$$

where $E(z)$, $\sigma_Y(z)$ and $E_t(z)$ are respectively the effective Young's modulus, yield stress and tangent modulus of the FGM; E_c and E_m are Young's moduli of ceramic and metal constituents, respectively; E_0, σ_{Ym} are the tangent modulus and yield stress of the metal, and the parameter q is the ratio of stress to strain transfer between the two material constituents, defined as

$$q=\frac{\sigma_c-\sigma_m}{|\varepsilon_c-\varepsilon_m|},\ 0<q<+\infty \tag{3}$$

The value of q depends on the properties of constituent materials and the microstructural interaction in the composite. Various values of q for FGMs formed from different ceramics and metals are given in the papers by Gunes *et al.* (2011), Huang *et al.* (2014). In the present work, SiC and Aluminum (Al) with properties listed in Table 1 are employed as ceramic and metal phases of the FGM beam. This Al/SiC FGM has q=91.6 GPa, which has been experimentally determined by Bhattacharyya *et al.* (2007). Fig. 2 shows the variation of the Young's modulus and the yield stress in the beam thickness direction of the Al/SiC FGM beam according to Eq (2).

Young's modulus of the FGM defined by Eq. (2) is not symmetrical with respect to the midplane of the beam. As a result, the neutral axis of the beam is no longer on the midplane, but it

Table 1 Material properties of Al and SiC

Materials	Young's modulus (GPa)	Yield stress (MPa)
Al	67	24
SiC	302	From Eq. (2)

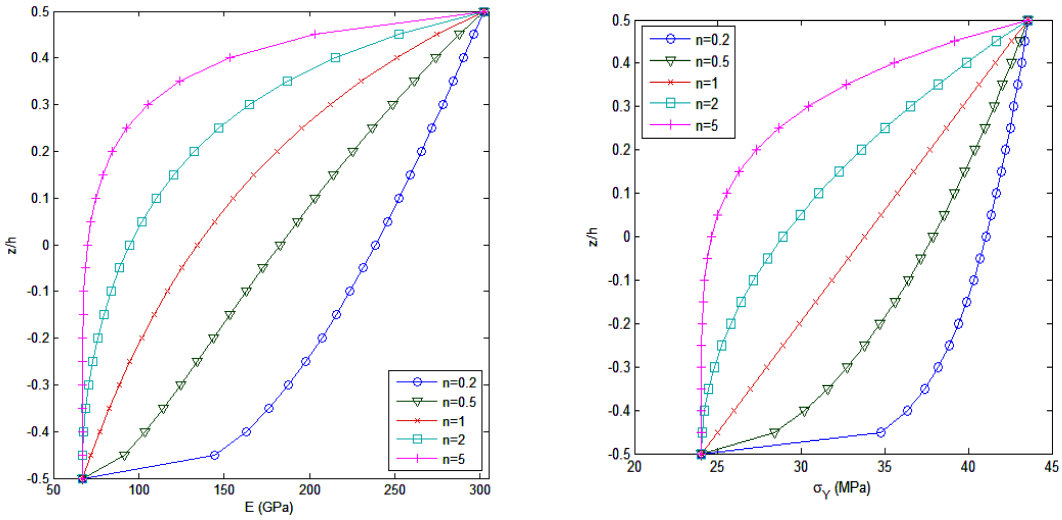

Fig. 2 Variation of Young's modulus and yield stress in thickness of Al/SiC FGM beam

shifts from this plane a distance h_0 (see Fig. 1), which can be determined by requiring the axial resultant on a section vanishes (Levyakov, 2013)

$$N = \int_A \sigma_x dA = 0, \text{ then } \quad h_0 = \frac{\int_{-h/2}^{h/2} E(z) z dz}{\int_{-h/2}^{h/2} E(z) dz} \tag{4}$$

where σ_x denotes the axial stress of beam under pure bending. It should be noted that with the Young's modulus given by Eq. (2), the integrals in Eq. (4) are not able compute explicitly. Simpson's rule is employed herewith in the determination of h_0.

The elastic foundation is assumed to be a nonlinear model with its reaction force is given by Rajasekhara and Venkateswara (1996)

$$r(x) = k_L w + k_{NL} w^3 \tag{5}$$

where w is the transverse displacement of the beam; K_L and K_{NL} are the linear and nonlinear foundation stiffness, respectively.

3. Finite element formulation

This section derives the finite element formulation for the buckling analysis of the FGM beam. The element is assumed to be initially straight and has a rectangular cross section. The bonding between the beam and the foundation is assumed to be perfect, and the beam does not lift off from the foundation. Based on the classical beam theory, displacements in x, y, z directions at any point in the beam are given by

$$\begin{aligned} u_1(x,z) &= u(x) - (z-h_0)w_{,x} \\ u_2(x,z) &= 0 \\ u_3(x,z) &= w(x) \end{aligned} \tag{6}$$

where $(.)_{,x}=\partial(.)/\partial x$ and h_0 is defined by Eq. (4).

The vector of nodal displacement for a two-node beam element, (i, j), can be written as

$$\mathbf{d}^T = \left\{\mathbf{u}^T \ \ \mathbf{w}^T\right\} \ \text{ with } \ \mathbf{u}^T = \left\{u_i \ \ u_j\right\},\ \mathbf{w}^T = \left\{w_i \ \ \theta_i \ \ w_j \ \ \theta_j\right\} \tag{7}$$

where and hereafter, a superscript 'T' denotes the transpose of a vector or a matrix. It should be noted that the order of the nodal displacements is not necessary as in Eq. (7), but it is convenient to separate the stretching and bending nodal displacements.

A bilinear stress-strain relation with isotropic hardening is assumed for the metal phase. The elastoplastic behavior of the FGM with the effective properties evaluated by Eq. (2) also follows a bilinear model, and this model represented by the elastoplastic modulus $\tilde{E}(z)$, defined as

$$\tilde{E}(z) = \begin{cases} E(z) & \text{if } \ |\sigma_x(z)| \le \sigma_Y(z) \ \text{ or unloading} \\ E_t(z) & \text{if } \ |\sigma_x(z)| > \sigma_Y(z) \end{cases} \tag{8}$$

where σ_x is axial stress, and $E(z)$, $E_t(z)$, $\sigma_Y(z)$ defined by Eq. (2).

The element formulation, namely the internal nodal force vector $\mathbf{f}_{in}$ and the tangent stiffness matrix $\mathbf{k}_i$ can be derived from the expression of the internal virtual work. For a beam element with length of l, the internal virtual work is a contribution from the beam bending and the foundation deformation as

$$\delta W_{in} = \int_V \sigma_x \delta\varepsilon_{xv} dV + \int_0^l r(x)\delta w_v dx \tag{9}$$

where the subscript 'v' stands for the "*virtual*"; V is the element volume; $\delta\varepsilon_v$ is the small virtual axial strain, and δw_v is the virtual transverse displacement.

Linear and cubic polynomials can be adopted to interpolate the axial and transverse displacements as

$$u = \mathbf{N}_u^T\mathbf{u},\ w = \mathbf{N}_w^T\mathbf{w} \tag{10}$$

with

$$\begin{aligned} \mathbf{N}_u^T &= \frac{1}{2}\left\{(1-\xi) \ \ (1+\xi)\right\} \\ \mathbf{N}_w^T &= \left\{\frac{1}{4}\left(2-3\xi+\xi^3\right) \ \ \frac{1}{8}l\left(\xi^2-1\right)(\xi-1) \ \ \frac{1}{4}\left(2+3\xi-\xi^3\right) \ \ \frac{1}{8}l\left(\xi^2-1\right)(\xi+1)\right\} \end{aligned} \tag{11}$$

where $\xi=2x/l-1$ is the dimensionless parameter, and with $0\le x\le l$, then $-1\le\xi\le 1$.

The nonlinear von Kármán strain-displacement relationship is employed for the axial strain ε_x as

$$\varepsilon_x = u_{,x} + \frac{1}{2}w_{,x}^2 + (z-h_0)\chi \tag{12}$$

where $\chi=-w_{,xx}$ is the beam curvature, z is the distance from the considered point to the midplane.

However, the beam element based on the interpolation functions (11) and the axial strain (12) encounters the membrane locking (Crisfield 1991). To overcome this problem, the membrane strain in Eq. (12) should be replaced by an effective ε_{eff}, defined as (Crisfield 1991)

$$\varepsilon_{eff} = \frac{1}{l}\int_0^l \left[\frac{\partial u}{\partial x} + \frac{1}{2}\left(\frac{\partial w}{\partial x}\right)^2\right] dx \tag{13}$$

Given Eqs. (10), (11) and (13), the axial strain in Eq. (12) can be written in the form

$$\varepsilon_x = \mathbf{b}_u^T \mathbf{u} + \frac{1}{2l}\mathbf{w}^T \int_0^l \mathbf{b}_w \mathbf{b}_w^T dx \mathbf{w} + (z - h_0)\mathbf{c}_w^T \mathbf{w} \tag{14}$$

in which

$$\begin{aligned}
\mathbf{b}_u^T &= \frac{\partial \mathbf{N}_u^T}{\partial x} = \frac{\partial \mathbf{N}_u^T}{\partial \xi}\frac{\partial \xi}{\partial x} = \frac{1}{l}\{-1 \quad 1\} \\
\mathbf{b}_w^T &= \frac{\partial \mathbf{N}_w^T}{\partial x} = \frac{1}{4l}\left\{6(\xi^2-1) \quad l(3\xi^2-2\xi-1) \quad -6(\xi^2-1) \quad l(3\xi^2+2\xi-1)\right\} \\
\mathbf{c}_w^T &= -\frac{\partial^2 w}{\partial x^2} = -\frac{1}{l^2}\{6\xi \quad l(3\xi-1) \quad -6\xi \quad l(3\xi+1)\}
\end{aligned} \tag{15}$$

From Eqs. (14) and (15), one can compute

$$\delta\varepsilon_{xv} = \mathbf{b}_u^T \delta\mathbf{u}_v + \left[\mathbf{e}_w^T + (z - h_0)\mathbf{c}_w^T\right]\delta\mathbf{w}_v \tag{16}$$

where

$$\mathbf{e}_w = \begin{Bmatrix} 36(w_i - w_j) + 3l(\theta_i + \theta_j) \\ 3l(w_i - w_j) + l^2(4\theta_i - \theta_j) \\ -\left[36(w_i - w_j) + 3l(\theta_i + \theta_j)\right] \\ 3l(w_i - w_j) + l^2(-\theta_i + 4\theta_j) \end{Bmatrix} \tag{17}$$

is the vector stemming from the nonlinear part of the axial strain.

The arbitrary axial and transverse displacements in Eq. (10) which make use shape functions in Eq. (11) can be obtained from the nodal displacement vectors in Eq. (7). By omitting the second term (distributed loading along the beam axis) of the internal virtual work in Eq. (9) and substituting the axial strain at the arbitrary point along the beam which can be calculated by using Eq. (14), we can write the internal virtual force defined in the form

$$\delta W_{in} = \int_V \sigma_x \delta\varepsilon_{xv} dV = \mathbf{f}_{in}^T \delta\mathbf{d}_v = \left\{\mathbf{f}_u^T \quad \mathbf{f}_w^T\right\}\left\{\delta\mathbf{u}_v \quad \delta\mathbf{w}_v\right\} \tag{18}$$

where $\mathbf{f}_u$ and $\mathbf{f}_w$ respectively denote the nodal internal forces corresponding to the nodal displacements $\mathbf{u}$, $\mathbf{w}$, and they have the forms

$$\begin{aligned}
\mathbf{f}_u^T &= \frac{l}{4}\int_{-1}^{1}\int_{-1}^{1} \sigma_x A \mathbf{b}_u^T d\xi d\eta \\
\mathbf{f}_w^T &= \frac{l}{4}\int_{-1}^{1}\int_{-1}^{1} \sigma_x A\left[\mathbf{e}_w^T + \left(\frac{h}{2}\eta - h_0\right)\mathbf{c}_w^T\right] d\xi d\eta + \frac{l}{2}\int_{-1}^{1} k_L w \mathbf{N}_w^T d\xi + \frac{l}{2}\int_{-1}^{1} k_{NL}\left(w\mathbf{N}_w^T\right)^3 d\xi
\end{aligned} \tag{19}$$

where $A=bh$ is the beam section area, and the dimensionless parameter, $\eta = \frac{2}{h}z$, is introduced for the purpose of evaluating the integrals numerically. The last two terms in Eq. (19) is the internal nodal forces due to the foundation deformation.

The element tangent stiffness matrix is obtained by differentiating the nodal force vector in Eq. (19) with respect to the nodal displacements as

$$\mathbf{k}_t = \begin{bmatrix} \mathbf{k}_{uu} & \mathbf{k}_{uw} \\ \mathbf{k}_{wu} & \mathbf{k}_{ww} \end{bmatrix} = \begin{bmatrix} \frac{\partial \mathbf{f}_u}{\partial \mathbf{u}} & \frac{\partial \mathbf{f}_u}{\partial \mathbf{w}} \\ \frac{\partial \mathbf{f}_w}{\partial \mathbf{u}} & \frac{\partial \mathbf{f}_w}{\partial \mathbf{w}} \end{bmatrix} \tag{20}$$

in which the $\boldsymbol{k}_{uu}$ and $\boldsymbol{k}_{ww}$ are the stiffness matrices stemming from element stretching and bending, respectively; $\boldsymbol{k}_{uw}=\boldsymbol{k}_{wu}^T$ is the stiffness resulted from the stretching-bending coupling. The expressions for these sub-matrices are as follows

$$\begin{aligned}
\mathbf{k}_{uu} &= \frac{l}{4}\int_{-1}^{1}\int_{-1}^{1} \tilde{E}A\mathbf{b}_u\mathbf{b}_u^T d\xi d\eta \\
\mathbf{k}_{uw} = \mathbf{k}_{wu} &= \frac{l}{4}\int_{-1}^{1}\int_{-1}^{1} \tilde{E}A\mathbf{b}_u\left[\mathbf{e}_w^T + \left(\frac{h}{2}\eta - h_0\right)\mathbf{c}_w^T\right] d\xi d\eta \\
\mathbf{k}_{ww} &= \frac{l}{4}\int_{-1}^{1}\int_{-1}^{1}\left\{\tilde{E}A\left[\mathbf{e}_w\mathbf{e}_w^T + \left(\frac{h}{2}\eta - h_0\right)^2 \mathbf{c}_w\mathbf{c}_w^T\right] + \sigma_x A\mathbf{B}\right\} d\xi d\eta + \frac{l}{2}\int_{-1}^{1} k_L N_w N_w^T d\xi + \frac{l}{2}\int_{-1}^{1} k_{NL}\left(N_w N_w^T\right)^3 d\xi
\end{aligned} \tag{21}$$

in which matrix **B** is given by

$$\mathbf{B} = \frac{\partial \mathbf{e}_w}{\partial \mathbf{w}} = \frac{1}{30l^2}\begin{bmatrix} 36 & 3l & -36 & 3l \\ 3l & 4l^2 & -3l & -l^2 \\ -36 & -3l & 36 & -3l \\ 3l & -l^2 & -3l & 4l^2 \end{bmatrix} \tag{22}$$

Since the axial stress σ_x varies in both the x and z directions, and the elastoplastic modulus $\tilde{E}$ ($\underline{z}$) is a function of z, Gauss quadrature is employed in computing the integrals in Eqs. (19) and (21). In addition, a simple algorithm for the one-dimensional elastoplastic problem described by Cook *et al.* (1991) is employed herein in updating the axial stress.

4. Numerical procedure

The formulated element internal force vector and tangent stiffness matrix are assembled to construct structural equilibrium equations, which can be written in the form (Crisfield, 1991)

$$\mathbf{g}(\mathbf{p}, \lambda) = \mathbf{q}_{in}(\mathbf{p}) - \lambda \mathbf{f}_{ef} \tag{23}$$

where the out-of-balance force vector **g** is a function of the current structural nodal displacements **p** and the load level parameter λ; $\mathbf{q}_{in}$ is the structural nodal force vector, assembled from the element force vector $\mathbf{f}_{in}$; $\mathbf{f}_{ef}$ is the fixed external loading vector. Since the eccentric load P is

statically equivalent to a centric load P plus a moment $M=Pe$, the axial loads and moments at the element nodes have the same amplitude, but in opposite sign, and these loads and moments are offset by the loads and moments from the neighbouring elements, so that the external load vector $\lambda\mathbf{f}_{ef}$ contains only the axial load P and the bending moment M at the beam ends. The system in Eq. (23) can be solved by an incremental/iterative procedure based on the Newton-Raphson method. In order to handle the complex nonlinear behavior such as the limit points, snap-though or snap-though behavior the arc-length control method developed by Crisfield (1991) is employed herein.

5. Numerical investigation

An FGM beam composed of SiC and Al with L=5 m; b=0.2 m; and h=0.1 m is employed in the numerical investigation in this section. Different values of tangent modulus for Al are available in the literature, and the computations reported below are carried out with $E_0=0.2E_m$. Gauss quadrature with nine points in the beam thickness and five points along the element length is employed in computing the element nodal force vector and tangent stiffness matrix. The beam is discretized by ten uniform elements. Two kinds of boundary conditions, namely clamped-free (CF) and simply-supported (SS) are considered. In order to facilitate the numerical discussion, the following dimensionless parameters which will be called the linear and nonlinear foundation parameters below, respectively are introduced

$$k_1 = k_L \frac{L^4}{E_m I} \quad , \quad k_3 = k_{NL} \frac{L^6}{E_m I} \tag{24}$$

The eccentric ratio $r_C=ec/r^2$ with $c=h/2-h_0$ and r is the radius of gyration, as introduced by Gere and Timoshenko (1991), is again adopted herein.

5.1 Formulation verification

In case of homogeneous beams resting on a linear elastic foundation, the finite element formulation given by Eqs. (19) and (21) deduce exactly to the one previously derived by Nguyen and his co-workers (2012). Since there is no data on the elastoplastic response of FGM beams, the validation of the formulations is confirmed by comparing the response of an elastic FGM beam to an eccentric axial load. Fig. 3 shows the load-displacement curves for the Al/SiC cantilever beam under an eccentric tip load with $e=h/2-h_0$ obtained by the present element, where for the sake of comparison, the result obtained by using the co-rotational element derived by Nguyen (2014) is also shown by the dashed lines. In the figure, the tip axial and transverse displacements, u and w, respectively are normalized by the beam length L, and the applied load is normalized by the Euler load of the cantilever full metal beam, that is $P_{cr}=\pi^2E_mI/4L^2$. For the elastic analysis herein, the yield stress of the metal phase is set to a large value, and thus the yielding will not occur. Regardless of the exponent n, a good agreement is noted from the figure. It should be noted that the effective Young's modulus in the work by Nguyen (2014) was evaluated by using Voigt model, namely

$$E(z) = (E_c - E_m)\left(\frac{z}{h} + \frac{1}{2}\right)^n + E_m \tag{25}$$

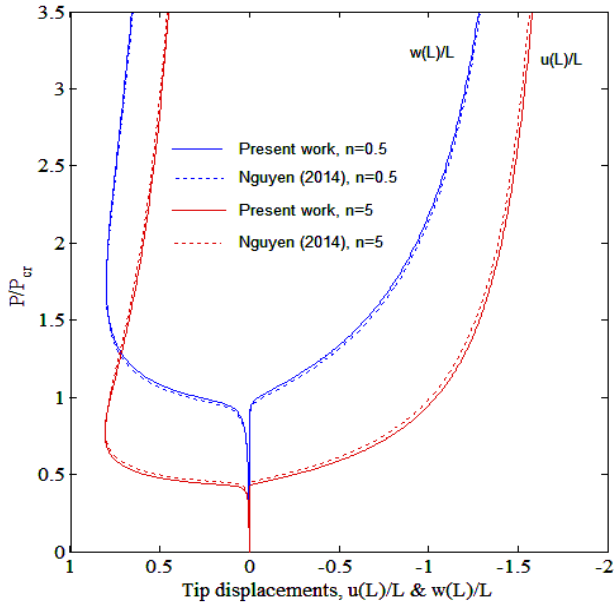

Fig. 3 Load-displacement curves for elastic FGM cantilever beam under an axial load

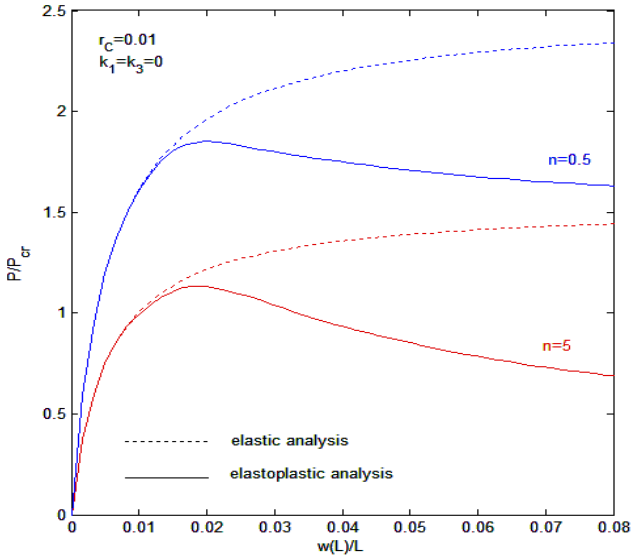

Fig. 4 Load-displacement curves of CF beam obtained by elastic and elastoplastic analyzes

which is slightly different from the one computed by Eq. (2).

5.2 Cantilever beam

In Fig. 4, the load-displacement curves represented the equilibrium paths of the CF beam without the foundation support obtained by the elastic and elastoplastic analyzes are depicted for

r_C=0.01, and for two values of the fraction exponent n=0.5 and n=5. In the figure, as in Fig. 3, P_{cr} is the Euler buckling load of the Al beam. The effect of plastic deformation is clearly seen from the figure, and as in case of the homogeneous beams (Nguyen *et al.*, 2012), the post-buckling of the FGM beam changes from stable to unstable when the effect of plastic deformation is taken into account. The effect of the material distribution is also clearly seen from the figure, where the post-buckling strength of the beam, measured in term of the ratio between the applied load P and the critical load P_{cr}, is higher for the beam associated with the lower exponent n. In other words, the post-buckling strength of the elastoplastic FGM beam is higher for the beam associated with a higher ceramic content.

The effect of the linear and nonlinear foundation parameters is illustrated in Figs. 5 and 6 for an eccentric ratio r_C=0.01 and an exponent n=5, respectively. The limit point of the beam, as seen from Fig. 5, increase considerably by increasing the linear foundation stiffness, but the post-buckling strength of the beam is hardly recognized. On the other hand, the nonlinear foundation parameter, as seen in Fig. 6 contributes to an increase in the post-buckling strength, but it hardly alters the limit load of the beam. In Fig. 7, the load-displacement curves of the CF beam resting on a nonlinear elastic foundation obtained by the elastic and elastoplastic analyses are depicted for two values of the exponent n=0.5 and n=5, and for r_C=0.01, k_1=20 and k_1=10. As in Fig. 4, the post-buckling strength of the beam on the elastic foundation is higher for the beam associated with a lower exponent n. The post-buckling strength of the beam is, however slightly improved by the foundation support.

To investigate the effect of plastic deformation on the behavior of the beam in more detail, the stresses and strains at lower and upper Gauss points near the clamped end at various values of the applied load are given in Table 2. The z co-ordinate of the lower and upper points are respectively -0.0484 m and 0.0484 m for the Gauss quadrature used herein (five points along the element

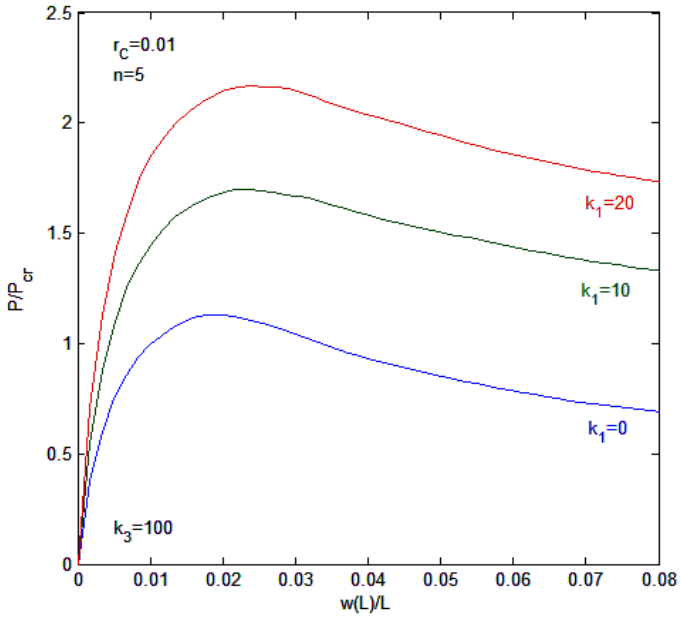

Fig. 5 Effect of linear foundation parameter on elastoplastic response of CF beam

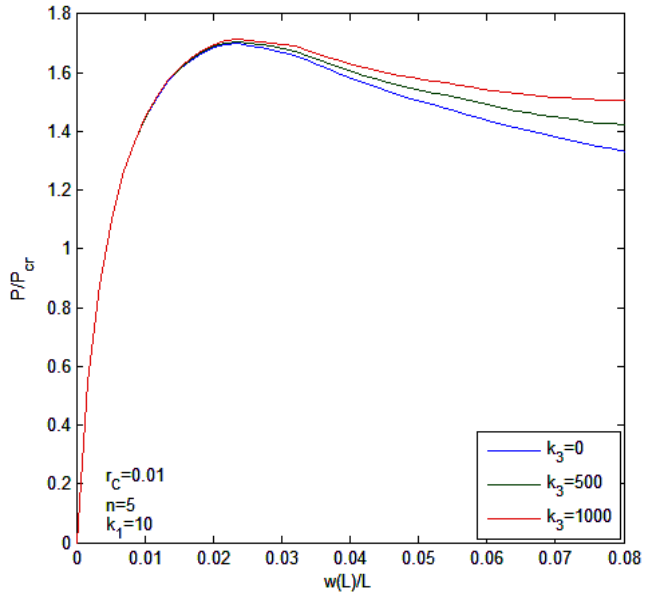

Fig. 6 Effect of nonlinear foundation parameter on elastoplastic response of CF beam

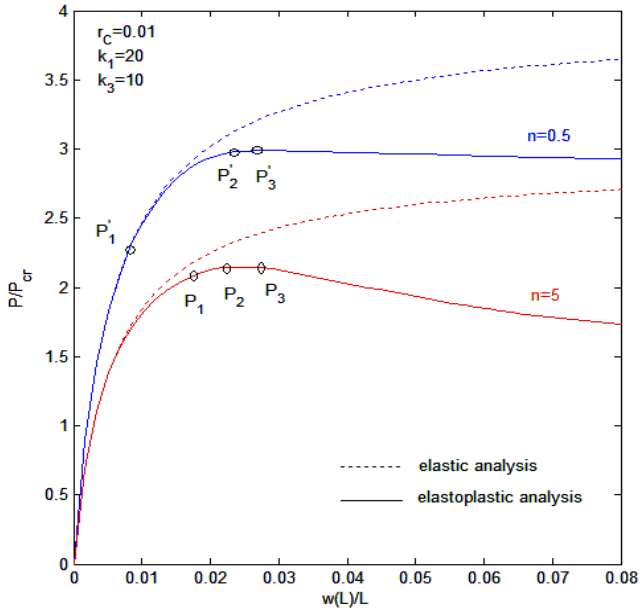

Fig. 7 Load-displacement curves for CF beam resting on a nonlinear elastic foundation obtained by elastic and elastoplastic analyzes

length and nine points through the thickness). The *x* co-ordinate is 0.0235m for both the points. Since these points are near the metal and ceramic surfaces, for the sake of convenient, the subscripts "*M*" and "*C*" are used to denote the stress and strain at the points. The stresses

Table 2 Axial stress and strain at lower and upper Gauss points corresponding the points P_i, P'_i (i=1..3) on the curves in Fig. 7

Foundation parameter	N	Loading Stages	P/P_{cr}	σ_M (10^7)	σ_C (10^7)	ε_M (10^{-4})	ε_C (10^{-4})
				(2.7125)	(4.3340)		
	0.5	P_1'	2.4674	0.9244	-5.8667	1.1045	-2.0036
		P_2'	2.9887	2.8862	-12.607	4.0498	-4.3466
$k_1 = 20$		P_3'	2.9877	2.9428	-13.080	4.3135	-4.5111
$k_3 = 10$				(2.4000)	(4.1220)		
	5	P_1	2.1460	0.9764	-7.4189	1.4574	-3.3631
		P_2	2.1480	1.0499	-7.6266	1.5670	-3.4677
		P_3	2.1467	1.1144	-7.8056	1.6632	-3.5580

Note: the values inside the brackets show the initial yield stresses of "M" and "C" for different values of the exponent n.

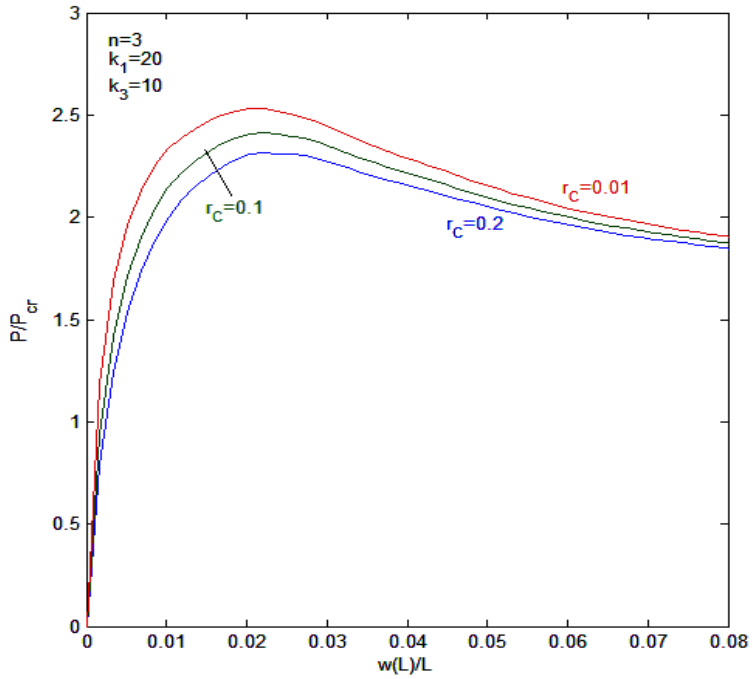

Fig. 8 Effect of eccentric ratio on the elastoplastic response of CF beam on nonlinear elastic foundation

highlighted in red color corresponding to the applied loading stages where yielding at the point has already occurred. As seen in Table 2, the yielding occurs in FGM beam is very different from that of the homogeneous beams where the top and bottom fibers yield symmetrically about the neutral axis at the mid-height of the cross section. In FGM beam, at a given value of the applied load, the stress amplitude near the ceramic surface is considerably higher than that near the metal surface while the strain is on the opposite side. The stresses at the applied loading stages P'_1, P_1, P_2 and P_3

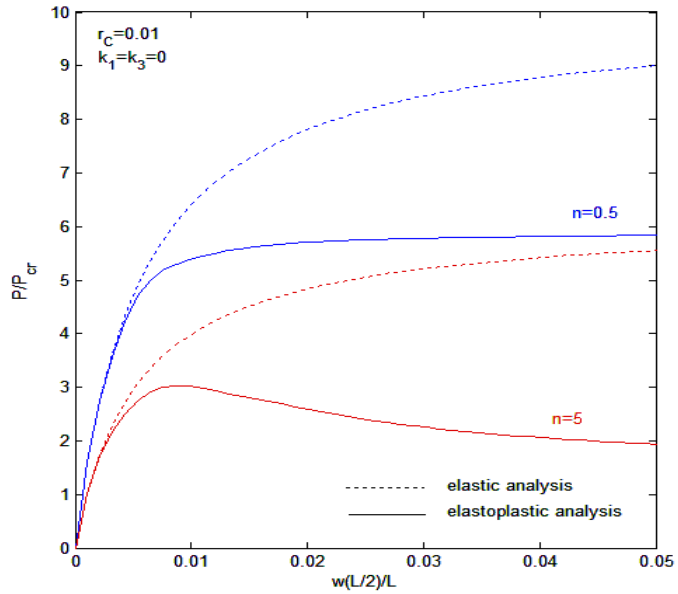

Fig. 9 Load-displacement curves of SS beam obtained by elastic and elastoplastic analyzes

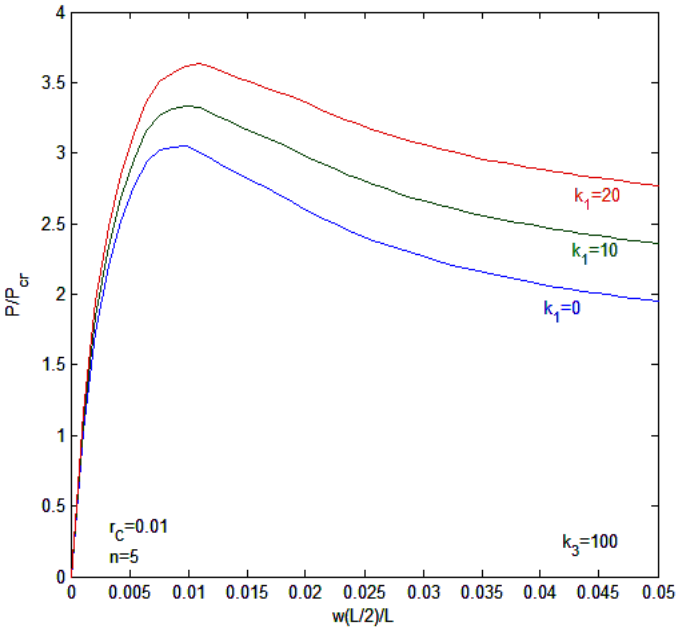

Fig. 10 Effect of linear foundation parameter on elastoplastic response of SS beam

in Table 2 show that yielding has occurred in the layer near the ceramic surface, but it has not occurred in a layer near the metal surface. This result is totally different from the homogeneous beam, where the yielding occurs in the lower and upper surfaces at the same time.

The effect of the eccentric ratio on the elastoplastic response of the CF beam is illustrated in

Fig. 8 for an exponent value n=3, and for k_1=20, k_3=10. The effect of the eccentric ratio on the elastoplastic behavior in the post-buckling region of the CF beam is similar to that of the homogeneous beams (Nguyen *et al.* 2012), in which the limit load of the beam steadily reduces by increasing the eccentric ratio.

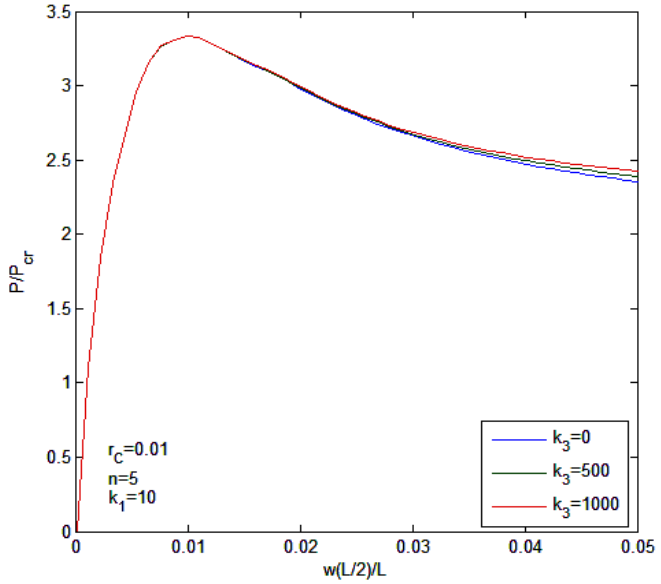

Fig. 11 Effect of nonlinear foundation parameter on elastoplastic response of SS beam

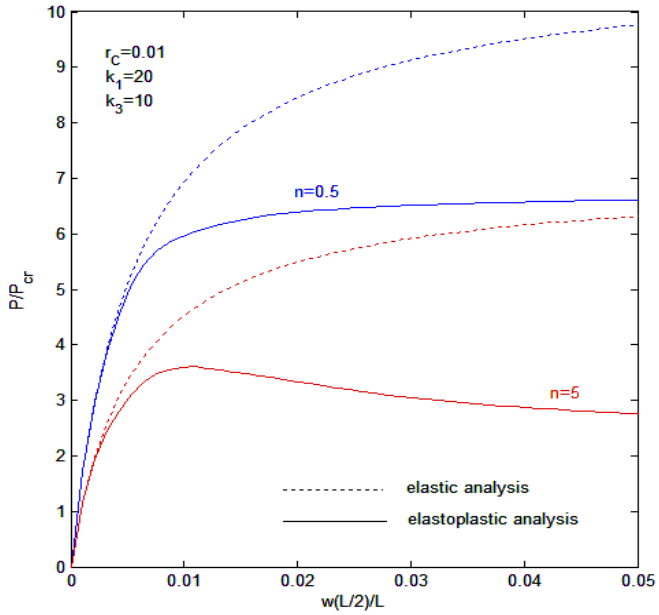

Fig. 12 Load-displacement curves for SS beam resting on a nonlinear elastic foundation obtained by elastic and elastoplastic analyzes

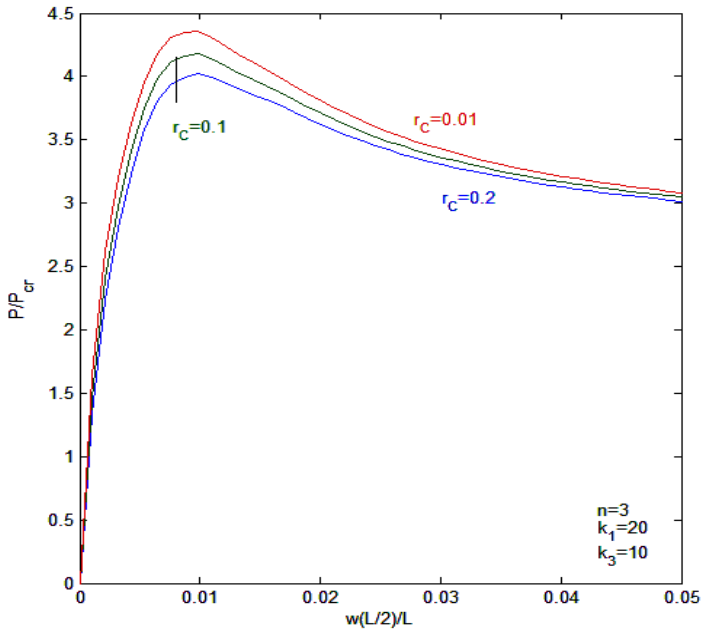

Fig. 13 Effect of eccentric ratio on the elastoplastic response of SS beam on nonlinear elastic foundation

5.3 Simply supported beam

In Fig. 9, the load-displacement curves of unsupported SS beam obtained by elastic and elastoplastic analyzes are depicted for r_C=0.01 and two values of the exponent n=0.5 and n=5. The effect of the foundation parameters, eccentric ratio for the SS beam is shown in Figs. 10-13. The effects of the plastic deformation, material distribution, linear foundation parameter, nonlinear foundation parameter, and eccentric ratio on the elastoplastic response of the SS beam is similar to that of the CF beam. However, comparing to the CF beam, the SS beam is less sensitive to the change in the foundation stiffness and the eccentric ratio.

6. Conclusions

The article investigated the elastoplastic response of FGM beams resting on a nonlinear elastic foundation to an eccentric axial load by using the finite element method. The formulation based on Euler-Bernoulli beam theory was derived by using the neutral surface as a reference plane. The TTO model was employed in evaluating the elastoplastic properties of the beam material. The nonlinear equilibrium equations have been solved by an incremental-iterative procedure in combination with the arc-length control method. Numerical examples are demonstrated for the beams with clamped-free and simply supported ends.

The numerical results are compared with the homogeneous case and the other material distribution for verifying the accuracy of the proposed formulation. The current formulation is verified by comparing the numerical results with the work by Nguyen (2012, 2014). Through the evaluations of Cantilever and Simply supported beam examples, the following conclusions can be

drawn:

- For different fraction exponent, *n*, the elastoplastic analyses curves show steady reduction of responses beyond the limit load compared to the elastic analyses results.
- The limit point of a beam increase considerably by increasing the linear foundation stiffness, *k*, but the post-buckling strength of the beam is hardly recognized in the nonlinear elastic foundation.
- The post-buckling strength of the beam is, however slightly improved by the type of foundation support (nonlinear elastic foundation).
- The effect of eccentric ratio, *r*, on the elastoplastic behavior in the post-buckling region of the beam is similar to that of the homogeneous beams.

It has been shown that yielding occurred in the FGM beam is very different from the homogeneous beam. The effects of the plastic deformation, material distribution, foundation parameters and eccentric ratio on the elastoplastic response of the FGM beams are studied and highlighted.

Acknowledgements

The authors would like to appreciate the valuable comments and discussions made by the reviewers. The work described in this paper has been supported by the Grants Nafosted 107.02-2015.02, VAST.HTQT.NGA.07/14-15 (Vietnam) and RFBR-14-01-93000 (Russia).

References

Bhattacharyya, M., Kapuria, S. and Kumar, AN. (2007), "On the stress to strain transfer ratio and elastic deflection behavior for Al/SiC functionally graded material", *Mech. Adv. Struct.*, **14**, 295-302.

Budkowska, B.B. and Szymczak, C. (1997), "Initial post-buckling behavior of piles partially embedded in soil", *Comput. Struct.*, **62**(5), 831-835.

Chaht, F.L., Kaci, A., Houari, M.S.A., Tounsi, A., Bég, O.A. and Mahmoud, S.R. (2015), "Bending and buckling analyses of functionally graded material (FGM) size-dependent nanoscale beams including the thickness stretching effect", *Steel Compos. Struct.*, **18**(2), 425-442.

Chakraborty, A., Gopalakrishnan, S. and Reddy, J.R. (2003), "A new beam finite element for the analysis of functionally graded materials", *Int. J. Mech. Sci.*, **45**, 519-539.

Chebl, C. and Neal, K.W. (1984), "A finite element method for elastic-plastic beams and columns at large deflections", *Comput. Struct.*, **18**(2), 255-261.

Chegenizadeh, A., Ghadimi, B., Nikraz, H. and Simsek, M. (2014), "A novel two-dimensional approach to modelling functionally graded beams resting on a soil medium", *Struct. Eng. Mech.*, **51**(5), 727-741.

Cook, R.D., Malkus, D.S. and Plesha, M.E. (1989), *Concepts and Applications of Finite Element Analysis*, 3rd edition. John Wiley & Sons, New York.

Crisfield, M.A. (1991), *Nonlinear Finite Element Analysis of Solids and Structures*, Volume 1, *Essentials*, John Wiley & Sons, Chichester.

Gere, J.M. and Timoshenko, S.P. (1991), *Mechanics of Materials*, 3rd Edition, Chapman & Hall, London.

Gunes, R., Aydin, M., Kemal, A.M. and Reddy, J.N. (2011), "The elasto-plastic impact analysis of functionally graded circular plates under low-velocities", *Compos. Struct.*, **93**(2), 860-869.

Hetényi, M. (1946), *Beams on Elastic Foundation: Theory with Applications in the Fields of Civil and Mechanical Engineering*, The University of Michigan Press, Ann Arbor.

Huang, H. and Han, Q. (2014), "Elastoplastic buckling of axially loaded functionally graded material

cylindrical shells", *Compos. Struct.*, **117**, 135-142.
Huang, Y. and Li, X.F. (2011), "Buckling analysis of non-uniform and axially graded beams with varying flexural rigidity", *ASCE J. Eng. Mech.*, **137**(1), 73-81.
Jahromi, B.H., Nayeb-Hashemi, H. and Vaziri, A. (2012), "Elasto-plastic stresses in a functionally graded rotating disk", *ASME J. Eng Mater-T*, **134**(2), 021004-021011.
Jin, Z.H., Paulino, G.H. and Dodds, R.H. (2003), "Cohesive fracture modeling of elastic–plastic crack growth in functionally graded materials", *Eng. Fract. Mech.*, **70**, 1885-1912.
Kadoli, R., Akhtar, K. and Ganesan, N. (2008), "Static analysis of functionally graded beams using higher-order shear deformation beam theory", *Appl. Math. Model.*, **32**(12), 2509-2525.
Kang, Y.A. and Li, X.F. (2009), "Bending of functionally graded cantilever beam with power- law nonlinearity subjected to an end force". *Int. J. Nonlin. Mech*., **44**(6), 696-703.
Kang, Y.A. and Li, X.F. (2010), "Large deflection of a non-linear cantilever functionally graded beam", *J. Reinf. Plast. Compos.*, **29**(4), 1761-1774.
Kadoli, R., Akhtar, K., and Ganesan, N. (2008), "Static analysis of functionally graded beams using higher order shear deformation beam theory", *Appl. Math. Model.*, **32**, 2509-2525.
Kounadis, A.N., Mallis, J. and Sbarounis, A. (2006), "Post-buckling analysis of columns resting on an elastic foundation", *Ach. Appl. Mech.*, **75**, 395-404.
Levyakov, S.V. (2013), "Elastica solution for thermal bending of a functionally graded beam", *Acta Mech*., **224**(8), 1731-1740.
Nguyen, D.K. (2004), "Post-buckling behavior of beam on two-parameter elastic foundation", *Int. J. Struct. Stab. Dyn.*, **4**(1), 21-43.
Nguyen, D.K., Trinh, T.H. and Gan, B.S. (2012), "Post-buckling response of elastic-plastic beam resting on an elastic foundation to eccentric axial load", *IES J. Pt. A: Civil Struct. Eng.*, **5**(1), 43-49.
Nguyen, D.K. (2013), "Large displacement response of tapered cantilever beams made of axially functionally graded material", *Compos. Pt. B Eng.*, **55**, 298-305.
Nguyen, D.K. (2014), "Large displacement behavior of tapered cantilever Euler-Bernoulli beams made of functionally graded material", *Appl. Math. Comput.*, **237**, 340-355.
Nguyen, D.K. and Gan, B.S. (2014), "Large deflections of tapered functionally graded beams subjected to end forces", *Appl. Math. Model.*, **38**(11-12), 3054-3066.
Nguyen, D.K., Gan, B.S. and Trinh, T.H. (2014), "Geometrically nonlinear analysis of planar beam and frame structures made of functionally graded material", *Struct. Eng. Mech.*, **49**(6), 727-743.
Patel, B.P., Ganapathi, M. and Touratier, M. (1999), "Nonlinear free flexural vibrations/post-buckling analysis of laminated orthotropic beams/columns on a two parameter elastic foundation", *Compos. Struct.*, **46**(2), 189-196.
Rajasekhara, N. N. and Venkateswara, R.G. (1996), "Free vibration and stability behavior of uniform beams and columns on nonlinear elastic foundation", *Comput. Struct.*, **58**(6), 1213-1215.
Razaqpur, A.G. and Shah, K.R. (1991), "Exact analysis of beams on two-parameter elastic foundations", *Int. J. Solid. Struct*., **27**(4), 435-451.
Tamura, I., Tomota, Y. and Ozawa, H. (1973), "Strength and ductility of Fe-Ni-C alloys composed of austenite and martensite with various strength", *Proceedings of the Third International Conference on Strength of Metals and Alloys*, Cambridge.
Zhang, Y., Huang, H. and Han, Q. (2015), "Buckling of elastoplastic functionally graded cylindrical shells under combined compression and pressure", *Compos. Pt. B Eng*., **69**, 120-126.
Zhaohua, F. and Cook, R.D. (1983), "Beam elements on two-parameter elastic foundations", *ASCE J. Eng. Mech.*, **109**(6), 1390-1402.